β-delayed γ-ray spectroscopy of non-yrast states in ^{138}Te near the neutron drip line

P. Lee,[1] C.-B. Moon,[2,*] C. S. Lee,[1,†] A. Odahara,[3] R. Lozeva,[4] A. Yagi,[3] S. Nishimura,[5] P. Doornenbal,[5] G. Lorusso,[5] P.-A. Söderström,[5] T. Sumikama,[6] H. Watanabe,[5] T. Isobe,[5] H. Baba,[5] H. Sakurai,[5] F. Browne,[5,7] R. Daido,[3] Y. Fang,[3] H. Nishibata,[3] Z. Patel,[5,8] S. Rice,[5,8] L. Sinclair,[5,9] J. Wu,[5,10] Z. Y. Xu,[11] R. Yokoyama,[12] T. Kubo,[5] N. Inabe,[5] H. Suzuki,[5] N. Fukuda,[5] D. Kameda,[5] H. Takeda,[5] D. S. Ahn,[5] D. Murai,[13] F. L. Bello Garrote,[14] J. M. Daugas,[15] F. Didierjean,[4] E. Ideguchi,[16] T. Ishigaki,[3] H. S. Jung,[17] T. Komatsubara,[18] Y. K. Kwon,[18] S. Morimoto,[3] M. Niikura,[5,11] I. Nishizuka,[6] and K. Tshoo[18]

[1]*Department of Physics, Chung-Ang University, Seoul, 156-756, Republic of Korea*
[2]*Department of Display Engineering, Hoseo University, Chung-Nam 336-795, Republic of Korea*
[3]*Department of Physics, Osaka University, Osaka 560-0043, Japan*
[4]*IPHC, CNRS, IN2P3 and University of Strasbourg, F-67037 Strasbourg Cedex 2, France*
[5]*RIKEN Nishina Center, Wako, Saitama 351-0198, Japan*
[6]*Department of Physics, Tohoku University, Sendai, Miyagi 980-8578, Japan*
[7]*School of computing engineering and mathematics, University of Brighton BN2 4JG, United Kingdom*
[8]*Department of Physics, University of Surrey, Guildford, GU2 7XH, United Kingdom*
[9]*Department of Physics, University of York, Heslington, York YO10 5DD, United Kingdom*
[10]*School of Physics and State key Laboratory of Nuclear Physics and Technology, Peking University, Beijing 100871, China*
[11]*Department of Physics, University of Tokyo, Tokyo 113-0033, Japan*
[12]*Center for Nuclear Study, University of Tokyo, RIKEN Campus, Wako, Saitama 351-0198, Japan*
[13]*Department of Physics, Rikkyo University, Tokyo 172-8501, Japan*
[14]*Department of Physics, University of Oslo N-0316, Norway*
[15]*CEA, DAM, DIF, F-91297 Arpajon Cedex, France*
[16]*RCNP, Osaka University, Osaka 567-0047, Japan*
[17]*Wako Nuclear Science Center (WNSC), Institute of Particle and Nuclear Studies (IPNS), High Energy Accelerator Research Organization (KEK), Wako, Saitama 351-0198, Japan*
[18]*Rare Isotope Science Project, Institute for Basic Science, Daejeon 305-811, Republic of Korea*

(Received 16 September 2015; published 21 October 2015)

We report on the first β-decay data of ^{138}Sb to ^{138}Te isotopes beyond the doubly magic ^{132}Sn. The parent nucleus was produced by the in-flight fission of a ^{238}U beam on a ^{9}Be target at 345 MeV per nucleon and measured at the BigRIPS separator of the Radioactive Isotope Beam Factory at RIKEN. By using advanced β-γ spectroscopy techniques, the half-life and the tentative spin-parity of ^{138}Sb were measured to be 346(19) ms and (3^-), respectively. In addition, we observed several low-lying non-yrast states in ^{138}Te for the first time. Our data allowed us to rearrange the positions of the first 2^+ and 4^+ states in this nucleus and to construct the level scheme of ^{138}Te in accordance with shell-model calculations. Additionally, we extend energy systematics of Te isotopes within neutron numbers 54 and 86.

DOI: 10.1103/PhysRevC.92.044320 PACS number(s): 23.40.−s, 21.10.Re, 21.60.Cs, 27.60.+j

I. INTRODUCTION

With two valence protons above the magic $Z = 50$, the Te isotopes are known to exhibit vibrational properties both below and beyond $N = 82$. For example, the majority of studies to investigate their nuclear structure (below $N = 82$) report on the coexistence of single-particle and collective structures [1–3].

In ^{136}Te, which has two neutrons above the $N = 82$ shell closure, an enhanced collectivity has been observed with the character of a spherical harmonic vibrator [4], which is in contrast to the two-neutron-hole ^{132}Te that has single particle behavior [5,6]. In a later study of the ^{136}Te nucleus, an anomaly in the transition strength between the ground state and the first 2^+ state has been found [7]. By using the quasiparticle random-phase approximation, this anomalous trend (for the neutron-rich Te beyond $N = 82$) was explained by a reduced pairing interaction [8].

Systematics of the excitation energy for the first 2^+ state $E(2^+)$ for the even-mass Te isotopes shows that $E(2^+)$ drastically decreases with increasing number of neutrons beyond $N = 82$. According to a recent large-scale shell-model calculation on the chain of Te and Xe nuclei, the neutron dominance in the wave function of excited states in neutron-rich Te isotopes is stronger, further suggesting that the Te nuclei beyond $N = 82$ undergo a drastic structural change [9].

^{138}Te, with two valence protons and four valence neutrons above the doubly magic ^{132}Sn has been studied only in prompt ^{248}Cm fission [10]. In comparison to BCS calculations, ^{138}Te was located in the transitional region where nuclear shape is expected to change from spherical in ^{136}Te to prolate in ^{140}Te [10]; however, experimental data on ^{138}Te and beyond

*cbmoon@hoseo.edu
†cslee@cau.ac.kr

 ©2015 American Physical Society

are severely limited. It is thus of a great interest to study ^{138}Te experimentally to elucidate its nuclear structure as well as to provide ingredients for the effective nucleon-nucleon interaction in the vicinity of the neutron drip line.

In the present study, we report the first spectroscopic results for ^{138}Te populated by the β decay of ^{138}Sb [$T_{1/2}$ = 350(15) ms [11]]. Moreover, because ^{138}Sb has a very large β-delayed neutron-emission probability of 72(8)%, ^{137}Te is likely also to be populated [11]. On the other hand, because the nucleus ^{139}Sb has an even larger β-delayed neutron-emission probability of 90(10)% [11], the delayed γ rays observed in the decay of ^{139}Sb also provide spectroscopic data on ^{138}Te, complementary to data obtained by the β decay of ^{138}Sb. In such a case, the initial spin when populating ^{139}Sb $\rightarrow$ ^{138}Te and ^{138}Sb $\rightarrow$ ^{138}Te is different, thus we can obtain unique access to certain spin states. Furthermore, β-decay spectroscopy of the respective odd-mass, ^{139}Sb and ^{137}Sb, channels will be reported elsewhere [12].

II. EXPERIMENT, ANALYSIS, AND RESULTS

The nuclei of interest were produced by in-flight fission of ^{238}U on a ^{9}Be target at 345 MeV/nucleon, separated by the BigRIPS separator at the Radioactive Isotope Beam Factory (RIBF) at the RIKEN Nishina Center [13]. The mean intensity of the primary beam was about 5 pnA over the course of the five days of beam time. Fission fragments, transported through a zero-degree spectrometer (ZDS), were unambiguously identified on the basis of the $B\rho$-ΔE-time-of-flight method [14]. And they were finally implanted into a wide-range active-silicon-strip stopper array for beta and ion detection (WAS3ABi), comprised of five layers of 1-mm-thick double-sided silicon-strip detectors (DSSSDs) [15]. It was surrounded by two 2-mm-thick plastic scintillators for the rejection of charge-exchange reactions. During the beam time, a total of 1.4×10^5 and 1.2×10^5 ions were collected for ^{138}Sb and ^{139}Sb, respectively. Emitted γ rays, following the β decay of Sb were then detected by the EUROBALL-RIKEN high-purity germanium (HPGe) cluster array (EURICA) [16] surrounding WAS3ABi.

To obtain the absolute photopeak efficiency for the EURICA array including WAS3ABi and the plastic scintillation counters, Monte Carlo simulations built by using the GEANT4 toolkit [17] were performed. Details about the detector configuration were considered and implemented as described in Refs. [15,16,18]. The simulation results were compared with the measured efficiencies at several points by using standard γ-ray sources. The add-back algorithm in Ref. [16] for reconstruction of Compton-scattered γ-ray was employed in calculating the absolute efficiency. It was found that the simulation reproduces within 5% uncertainty the experimental results, as shown in Fig. 1(a). Distributing the γ-ray emitters over the layers of the DSSSD detector, according to the experimental implantation pattern in Fig. 1(b), allowed us to compute the corrected efficiency curve [Simulation II in Fig. 1(a)]. It was further used to obtain the absolute γ-ray intensity in the analysis.

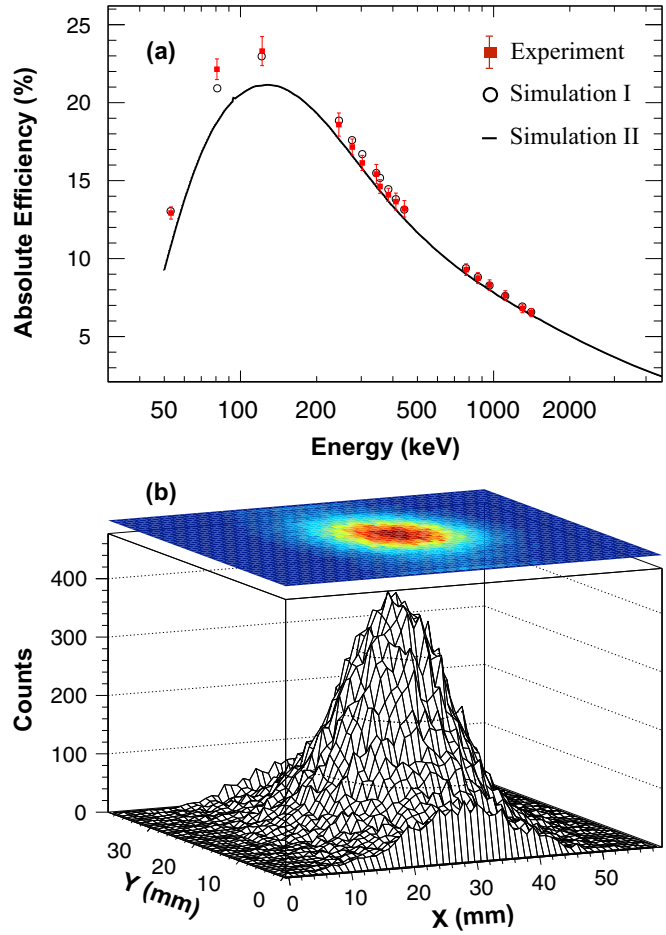

FIG. 1. (Color online) (a) Experimental and simulated absolute photopeak efficiency of the EURICA including ancillary detectors. Simulation I (open circles) and II (solid line) are for point sources at a fixed position and γ emitters distributed over the one of the DSSSD layers, respectively. (b) Implanted position distribution of ^{138}Sb accumulated in WAS3ABi.

Because the ions are slowed down before implantation, we detected a typical charge-exchange rejection rate of the order of 8%. This rejection was further used in the analysis.

In order to correlate the implanted heavy ions of interest with β particles recorded at one of the pixels in the DSSSD layers, we imposed constraints on both position and timing. For events in a singles mode, a β-decay event was considered in the implantation pixel. Up to 25 neighboring pixels were considered in a coincidence mode considering the position resolution of DSSSD stoppers. All β particles detected within certain time window (a multiple of half-life) after implantation were considered to be included in sorting. The resulting β-γ data is sorted into a β-correlated $\gamma\gamma$ matrix based on the their respective timing information.

Figure 2 illustrates the β-delayed γ-ray singles spectrum and coincidence spectra with energy gates on the transitions in ^{138}Te. The coincidence timing window was $\pm$200 ns considering that the average timing resolution of the EURICA is 200 ns. The two strong transitions seen in the singles spectrum are already known from Ref. [10] to belong to ^{138}Te.

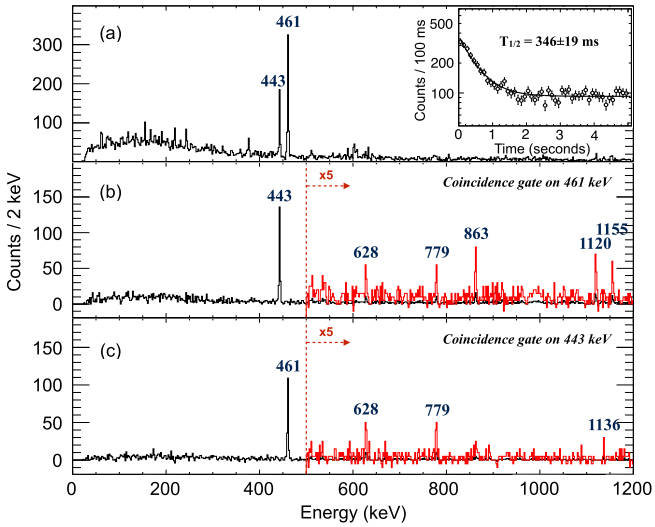

FIG. 2. (Color online) (a) β-delayed γ-ray singles spectrum of ^{138}Sb and (b), (c) its γ-ray coincidence spectra. The β-decay curve with a lifetime fit is shown in the inset.

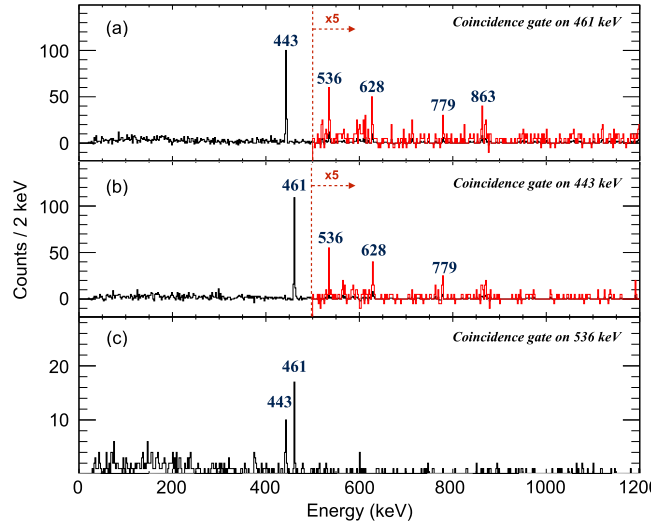

FIG. 3. (Color online) γ-ray coincidence spectra on transitions in ^{138}Te detected in the ^{139}Sb-βn decay. The gates are associated with (a) 460.8 keV, (b) 442.8 keV, and (c) 535.5 keV.

However, in the singles spectrum, the 460.8 keV transition, which was suggested to be a transition of $4^+ \rightarrow 2^+$ in Ref. [10], is approximately twice as intense as the 442.8 keV transition ($2^+ \rightarrow 0^+$), implying that the positions of the 460.8 and 442.8 keV transitions should be exchanged in the level scheme, thus corresponding to the $2^+ \rightarrow 0^+$ and $4^+ \rightarrow 2^+$ transitions, respectively. The unique selection rule (of the initial spin of ^{138}Sb) in our case gives the possibility to enhance the population of these two states. It is possible that, in the previous work [10], these γ rays were found with the same intensity as they were identified in triple coincidence mode with a partner nucleus, and all γ rays in the cascade would be of similar intensity. The doubled intensity in our case indicates that about half of the decay strength proceeds through the 4^+, while the other half proceeds through the 2^+ state.

The half-life of ^{138}Sb was deduced by using the identification with the 442.8 and 460.8 keV transitions. Half-lives with different energy gates were consistent with each other, and the weighted average of them amounts to 346(19) ms, in a good agreement with the previous measurement [11].

To search for new excited states in ^{138}Te, $\gamma\gamma$ coincidence data after the β decay of not only ^{138}Sb but also ^{139}Sb is complementarily analyzed. The γ-ray spectra associated with the β-delayed neutron decay of ^{139}Sb are also shown in Fig. 3. The β decays of ^{138}Sb and ^{139}Sb have a similar decay pattern due to the high neutron-emission probability of ^{139}Sb [11]. From the 271.0 keV transition, which is known to be the $(9/2^-) \rightarrow (7/2^-)$ transition in ^{139}Te [19], we deduced the ratio of I_{271} to I_{461} to be 9(2), consistent with the β-delayed neutron-emission probability of ^{139}Sb. We found different timing curves of the 460.8 keV line between the decay of ^{139}Sb with a half-life of 93 ms [11] and ^{138}Sb, again confirming that those originated from different parent nuclei. Moreover, the 535.5 keV transition, which is proposed as a $6^+ \rightarrow 4^+$ transition in ^{138}Te [10], is seen only in the coincidence spectrum after the β-delayed neutron emission of ^{139}Sb. This could be explained by the difference in the distribution of nuclear spins of ^{139}Sb with respect to those of ^{138}Sb, so that the 6^+ state in ^{138}Te could be accessible.

Energies and relative intensities for all of the observed γ transitions are summarized in Table I. In addition, β branches, which are computed by using γ-ray-intensity imbalances, and the corresponding log ft values are given in Table II. In the computation of β branches, internal conversion is ignored because no conversion electron is observed in an electron spectrum recorded by the WAS3ABi. As experimental-mass data for ^{138}Sb is not available, $Q(\beta^-) = 11.2(3)$ MeV [20] is used in the computation of log ft values, with LOGFT [21]. In order to prove the overall procedure, we compared log ft for the β decay of ^{145}Cs, deduced from the present experimental data and method, with the literature value [22]. However, it is worth mentioning that these log ft values should be taken as lower limits for transitions in this particular neutron-rich nucleus with a high $Q(\beta^-)$ value because of the pandemonium effect [23].

III. DISCUSSION

In the present study, several new excited states are observed for the first time. The present experimental data allows us to change the excitation energy of the first 2^+ state and rearrange the level scheme. The constructed level scheme is shown in Fig. 4 and is summarized as follows:

The 460.8 and 903.6 keV levels. In the previous study of ^{138}Te, the 442.8 keV transition was assigned as $E(2^+)$ in ^{138}Te. Based on the observed γ-ray intensity as well as coincidence relations, we assign the 460.8 and 442.8 keV transitions as the deexcitation energies of the 2^+ and 4^+ states, respectively. With these corrections, the ratio $E(4^+)/E(2^+)$ indicating the vibrational-like character of the low-lying collective states becomes 1.96, which is slightly lower than the previous value of 2.04 [10].

TABLE I. Characteristics of the observed γ-ray transitions in the present work.

E_γ (keV)	I_γ [a] [b]	J_i^π	E_i (keV)	J_f^π	E_f (keV)	Coincidences (keV)
460.8(5)	100	(2^+)	460.8(5)	0^+	0.0	442.8, 627.6, 778.5, 862.6, 1120.3, 1136.1, 1154.5
442.8(5)	40(3)	(4^+)	903.6(14)	(2^+)	460.8(5)	460.8, 627.6, 778.5
862.6(5)	7(1)	(2^+)	1323.4(16)	(2^+)	460.8(5)	460.8
1120.3(5)	5(1)	$(2^+,3^+,4^+)$	1581.1(19)	(2^+)	460.8(5)	460.8
1154.5(5)	6(1)	$(2^+,3^+,4^+)$	1615.3(19)	(2^+)	460.8(5)	460.8
535.5 (5)[c]		(6^+)	1439.1(26)	(4^+)	903.6(14)	442.8, 460.8
627.6(5)	6(1)	$(2^+,3^+,4^+)$	1531.2(27)	(4^+)	903.6(14)	442.8, 460.8
778.5(5)	3(1)	$(2^+,3^+,4^+)$	1682.1(28)	(4^+)	903.6(14)	442.8, 460.8
1136.1(5)	3(1)	$(2,^+3^+,4^+)$	2039.7(32)	(4^+)	903.6(14)	442.8, 460.8

[a]Relative intensities observed in the β decay of ^{138}Sb (except for the 535.5 keV transition) normalized to $I_{460.8}$. Quoted error includes statistical and 5% systematical error estimated from the γ-ray efficiency of the EURICA.
[b]Intensities above the first 4^+ excited state are deduced from the coincidence spectra with 442.8 and 460.8-keV-energy gates.
[c]Observed only in the β-delayed neutron decay.

The 1323.4, 1581.1, and 1615.3 keV levels. Three γ rays at 862.6, 1120.3, and 1154.5 keV were observed in coincidence with the $2^+ \rightarrow 0^+$ transition. According to the observed γ-ray intensity, we tentatively concluded that these γ rays feed the first 2^+ state. The 1323.3 keV level is assigned as the second 2^+ state based on the systematics of the second 2^+ states observed in the neighboring isotopes and isotones, and the 2_2^+ state predicted by the shell model [9].

The 1531.2, 1682.1, and 2039.7 keV levels. Three γ rays of 627.6, 778.5, and 1136.1 keV depopulating these excited states are observed in coincidence with the $4^+ \rightarrow 2^+$ and $2^+ \rightarrow 0^+$ transitions in ^{138}Te. Based on their relative intensities, the three new excited states are placed with possible spins of (2,3,4) with a positive parity based on the intensity ratios with the already-known low-lying 2^+ states.

The 1439.1 keV level. This excited state is depopulated by 535.5 keV transition and is interpreted in Ref. [10] as a $J^\pi = (6^+)$ member of the ground-state band. Assuming that this spin is correct, this state can possibly be populated only in the βn decay of ^{139}Sb. This experimental observation would be consistent with the 6^+ assignment.

Prior to our measurement, the spin-parity of the ground state in ^{138}Sb was not known. According to the feeding pattern observed in the present study, we may restrict the possible spin-parity values. The $\nu f_{7/2}$ orbital is the lowest in energy along the $N = 83$ isotonic chain for $Z = 50$ to 64 (Fig. 39 in Ref. [24]) and originates in a larger part the ground states also in the Te nuclei. It has been suggested that the lowest orbital in ^{137}Te and ^{139}Te is $\nu f_{7/2}$ [12,19,25] and can be considered in ^{138}Sb. The proton single-particle orbital also needs to be discussed because the relevant proton orbitals evolve dynamically with respect to the neutron number (Fig. 36 in Ref. [24]) in the doubly magic ^{132}Sn region. According to the available nuclear data for odd-mass $^{115-135}$Sb isotopes, $\pi g_{7/2}$ remains the lowest proton orbital in the $N = 72$ to 84 isotopes. The experimental excitation energy of $J^\pi = 5/2^+$ decreases with the neutron number; thus, assuming that these originate from the $\pi d_{5/2}$ and $\pi g_{7/2}$ orbitals one may expect that both influence the energy spectrum of ^{138}Sb. One may therefore expect that the ground state of ^{138}Sb contains mostly $\pi g_{7/2} \nu f_{7/2}$ and $\pi d_{5/2} \nu f_{7/2}$ configurations [9]. Therefore, the β decay of ^{138}Sb to low-lying states in ^{138}Te is likely to be the

TABLE II. Calculated β-branching ratios and corresponding log ft values for excited states populated in the β decay of ^{138}Sb. See text for details.

Energy (keV)	I_{β^-}	log ft
0		
460.8(5)	10.4(43)	6.3(2)
903.6(14)	7.0(29)	6.4(2)
1323.4(16)	1.9(5)	7.0(2)
1531.1(27)	1.3(5)	7.0(2)
1581.1(19)	1.1(5)	7.0(2)
1615.3(19)	1.3(5)	7.0(2)
1682.1(28)	0.6(3)	7.3(2)
2039.7(32)	0.6(3)	7.2(2)

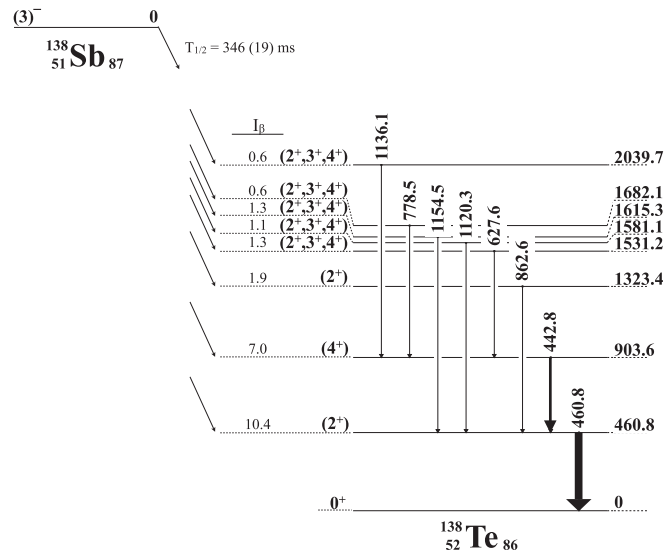

FIG. 4. New β-decay scheme for ^{138}Sb obtained in this work. All transitions shown are new except the 442.8 and the 460.8 keV lines, which are reordered with respect to the previous work [10].

$\nu f_{7/2} \rightarrow \pi g_{7/2}$ or $\nu f_{7/2} \rightarrow \pi d_{5/2}$ transition, both categorized as the first forbidden type. The parity of these configurations and the strong and equally distributed intensities of the β-decay branches to the respective (4^+) and (2^+) states in ^{138}Te support the (3^-) assignment of the ground state in ^{138}Sb. This is further reinforced with the calculated log ft values.

There are two facts that support low-spin nature of excited states observed in the present work and can support their assignment as non-yrast states. We emphasize that no transition, even the one between the first-excited state $J^{\pi}_{608} = 11/2^-$ and the ground state $J^{\pi}_{g.s.} = 7/2^-$ of ^{137}Te [25], is observed in the β-delayed γ-ray decay of ^{138}Sb, despite the large β-delayed neutron-emission probability. This observation could be attributed to the fact that the nuclear spins of low-lying states in ^{137}Te are relatively high so that the excited states in ^{137}Te can hardly be populated in the β-delayed neutron decay of ^{138}Te. Second, the computed log ft values lie in the range of the first forbidden transition. The β transitions to the excited states in ^{138}Te imply that these excited states are most likely with spins between 2 and 4. The positive parity can be supported by the fact that no strong Gamow–Fermi transition is observed in the β decay. The newly assigned levels with the suggested spin and parities are shown in Table I and Fig. 4.

We have examined nuclear structural change systematically in the Te isotopes. In the limit of a harmonic vibrator, the ratio of the first 4^+ to 2^+ energy, $E(4^+)/E(2^+)$, is 2, and $E(6^+)/E(2^+)$ corresponds to 3. The systematics of such values is shown in Fig. 5. The ratios for Te isotopes except near the $N = 82$ shell closure remain constant, indicating a spherical harmonic vibrator. It is worthwhile to note that a small minimum in the systematics of $E(6^+)/E(2^+)$ and $E(4^+)/E(2^+)$ at $N = 64$ indicates an effect of the subshell gap at neutron number of 64 [27]. On the contrary, the values of $E(6^+)/E(2^+)$ are gradually increasing toward 3 below $N = 82$ but steeply increase above $N = 82$. According to Ref. [2], the 6^+ level could be interpreted in terms of the $\pi(g_{7/2})^2$ aligned configuration in Te isotopes with $N < 82$. One can thus compare this with enhancement of $E(6^+)/E(2^+)$ in Te with $N > 82$ which is likely due to a large contribution by a pair of neutrons in the $\nu f_{7/2}$ orbital coupled with a pair of two protons in the $\pi g_{7/2}$ orbital [4].

In order to understand the structure of neutron-rich Te isotopes with $N > 82$ several theoretical works based on the shell model have been done [8,9,28,29]. The present level scheme, with a shell-model theory by Bianco *et al.* [9] are shown in Fig. 6. This large-scale shell-model approach was based on an iterative matrix diagonalization algorithm endowed with an important sampling which selects the basis states relevant to the eigenstates to be generated [9]. Focussing on the predictions of Ref. [9], we note that the neutron weight in the 2^+_1 states gets more enhanced in Te isotopes as they depart from the $N = 82$ shell closure toward the drip line. This result is understood as a neutron dominance in the neutron-proton exchange symmetry, generally preserved in most Te isotopes with neutron numbers below $N = 82$, and broken for the Te isotopes with $N > 84$. As can be seen in Fig. 6, the associated 2^+ states predicted by the theory well agree with our experimental results. Moreover, no negative-parity (e.g., 3^-) states are predicted by the theory,

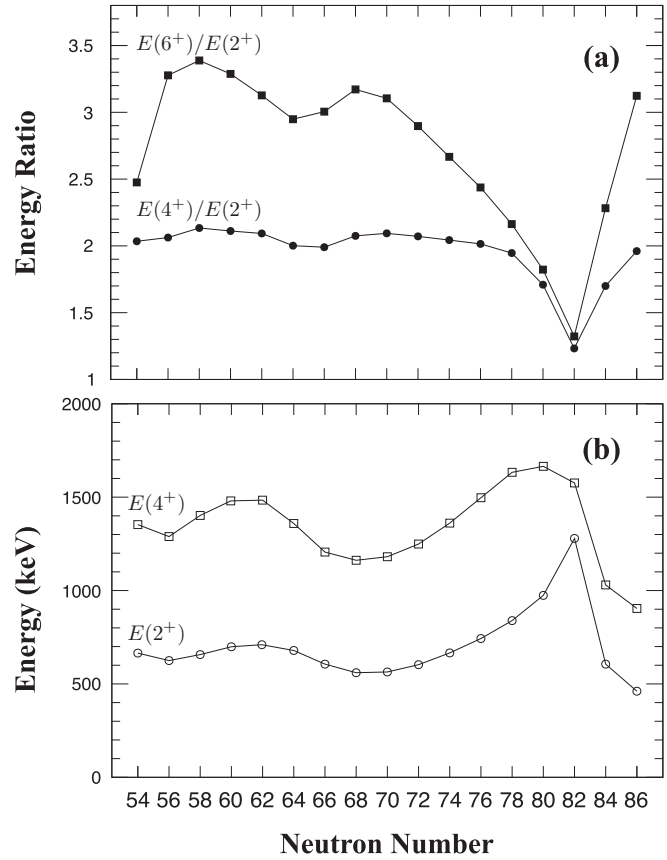

FIG. 5. Systematics for (a) the excitation-energy ratio $E(6^+)/E(2^+)$ and $E(4^+)/E(2^+)$, and (b) excitation energies $E(2^+)$ and $E(4^+)$ in Te isotopes from $N = 54$ to $N = 86$ [26] and the present work for ^{138}Te.

which supports the positive-parity assignments of the other observed states. It is interesting to find whether the non-yrast states observed above the 6^+ level correspond to the 2^+ states, associated with the mixed proton-neutron exchange nonsymmetry. According to the Monte Carlo shell-model

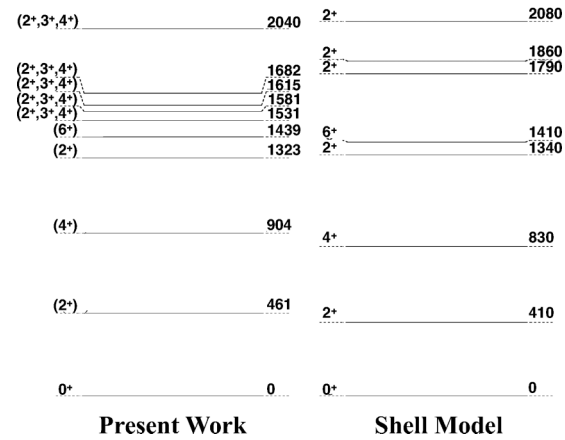

FIG. 6. Comparison between the experimental excitation energies from (a) the present work and (b) the theoretical values calculated by using the shell model [9].

study for Te with $N > 82$ [28], the structure of the 2_2^+ state can be explained as a mixed-symmetry state characterized by an antisymmetric wave function with respect to interchanges between proton pairs and neutron pairs. The existence of 1^+, 2_2^+, and 3^+ as the full set of the mixed-symmetry states were also predicted by the model. In this respect, the present non-yrast states offer experimental candidates for such 1^+, 2_2^+, and 3^+ mixed-symmetry states as well. In order to further support that, extensive future experimental measurements on the half-lives and transition multipolarities are required.

IV. CONCLUSION

In this work we investigated for the first time the β-decay scheme of ^{138}Sb to ^{138}Te. The half-life of the parent ^{138}Sb nucleus was measured to be 346(19) ms. We assigned for the first time the ground-state spin parity of ^{138}Sb to be $J^\pi = (3^-)$ based on the intensity balance and log ft values. In the newly constructed level scheme of the neutron-rich ^{138}Te nucleus, where we rearranged the position of the first 2^+ and 4^+ states, we also identified several non-yrast states. We discussed the new data in terms of shell-model calculations and outlined the evolution of nuclear-shell structure based on the energy systematics of Te isotopes along $N = 54$ and 86. The newly observed non-yrast states provide now a testing ground for the development of nuclear models.

ACKNOWLEDGMENTS

This work was carried out at the RIBF operated by RIKEN Nishina Center, RIKEN and CNS, University of Tokyo. We acknowledge the EUROBALL Owners Committee for the loan of germanium detectors and the PreSpec Collaboration for the readout electronics of the cluster detectors. Part of the WAS3ABi was supported by the Rare Isotope Science Project, which is funded by the Ministry of Science, ICT, and Future Planning (MSIP) and the National Research Foundation (NRF) of Korea. This research was partly supported by JSPS KAKENHI Grant No. 25247045 and the National Research Foundation Grant funded by the Korean Government (Grants No. NRF-2009-0093817 and No. NRF-2013R1A1A2063017). FR-JP LIA support is also acknowledged.

[1] C. S. Lee, J. A. Cizewski, D. Barker, R. Tanczyn, G. Kumbartzki, J. Szczepanski, J. W. Gan, H. Dorsett, R. G. Henry, and L. P. Farris, Nucl. Phys. A **528**, 381 (1991).

[2] C.-B. Moon, J. U. Kwon, S. J. Chae, J. C. Kim, S. H. Bhatti, C. S. Lee, T. Komatsubara, J. Mukai, T. Hayakawa, H. Kimura, J. Lu, M. Matsuda, T. Watanabe, and K. Furuno, Phys. Rev. C **51**, 2222 (1995).

[3] C.-B. Moon, T. Komatsubara, T. Shizuma, K. Uehiyama, N. Hashimoto, M. Katoh, K. Matsuura, M. Murasaki, Y. Sasaki, H. Takahashi, Y. Tokita, and K. Furuno, Z. Phys. A: Hadrons Nucl. **358**, 373 (1997).

[4] J. A. Cizewski, M. A. C. Hotchkis, J. L. Durell, J. Copnell, A. S. Mowbray, J. Fitzgerald, W. R. Phillips, I. Ahmad, M. P. Carpenter, R. V. F. Janssens, T. L. Khoo, E. F. Moore, L. R. Morss, Ph. Benet, and D. Ye, Phys. Rev. C **47**, 1294 (1993).

[5] R. O. Hughes, N. V. Zamfir, R. F. Casten, D. C. Radford, C. J. Barton, C. Baktash, M. A. Caprio, A. Galindo-Uribarri, C. J. Gross, P. A. Hausladen, E. A. McCutchan, J. J. Ressler, D. Shapira, D. W. Stracener, and C.-H. Yu, Phys. Rev. C **69**, 051303(R) (2004).

[6] M. Danchev, G. Rainovski, N. Pietralla, A. Gargano, A. Covello, C. Baktash, J. R. Beene, C. R. Bingham, A. Galindo-Uribarri, K. A. Gladnishki, C. J. Gross, V. Yu. Ponomarev, D. C. Radford, L. L. Riedinger, M. Scheck, A. E. Stuchbery, J. Wambach, C.-H. Yu, and N. V. Zamfir, Phys. Rev. C **84**, 061306(R) (2011).

[7] D. C. Radford, C. Baktash, J. R. Beene, B. Fuentes, A. Galindo-Uribarri, C. J. Gross, P. A. Hausladen, T. A. Lewis, P. E. Mueller, E. Padilla, D. Shapira, D. W. Stracener, C.-H. Yu, C. J. Barton, M. A. Caprio, L. Coraggio, A. Covello, A. Gargano, D. J. Hartley, and N. V. Zamfir, Phys. Rev. Lett. **88**, 222501 (2002).

[8] J. Terasaki, J. Engel, W. Nazarewicz, and M. Stoitsov, Phys. Rev. C **66**, 054313 (2002).

[9] D. Bianco, N. Lo Iudice, F. Andreozzi, A. Porrino, and F. Knapp, Phys. Rev. C **88**, 024303 (2013).

[10] F. Hoellinger, B. J. P. Gall, N. Schulz, W. Urban, I. Ahmad, M. Bentaleb, J. L. Durell, M. A. Jones, M. Leddy, E. Lubkiewicz, L. R. Morss, W. R. Phillips, A. G. Smith, and B. J. Varley, Eur. Phys. J. A **6**, 375 (1999).

[11] O. Arndt, K.-L. Kratz, W. B. Walters, K. Farouqi, U. Köster, V. Fedosseev, S. Hennrich, C. J. Jost, A. Wöhr, A. A. Hecht, B. Pfeiffer, J. Shergur, and N. Hoteling, Phys. Rev. C **84**, 061307 (2011).

[12] R. Lozeva *et al.* (unpublished).

[13] T. Kubo, D. Kameda, H. Suzuki, N. Fukuda, H. Takeda, Y. Yanagisawa, M. Ohtake, K. Kusaka, K. Yoshida, N. Inabe, T. Ohnishi, A. Yoshida, K. Tanaka, and Y. Mizoi, Prog. Theor. Exp. Phys. **2012**, 03C003 (2012).

[14] N. Fukuda, T. Kubo, T. Ohnishi, N. Inabe, H. Takeda, D. Kameda, and H. Suzuki, Nucl. Instrum. Methods Phys. Res., Sect. B **317**, 323 (2013).

[15] S. Nishimura, Prog. Theor. Exp. Phys. **2012**, 03C006 (2012).

[16] P.-A. Söderström, S. Nishimura, P. Doornenbal, G. Lorusso, T. Sumikama, H. Watanabe, Z. Y. Xu, H. Baba, F. Browne, S. Go, G. Gey, T. Isobe, H.-S. Jung, G. D. Kim, Y.-K. Kim, I. Kojouharov, N. Kurz, Y. K. Kwon, Z. Li, K. Moschner, T. Nakao, H. Nishibata, M. Nishimura, A. Odahara, H. Sakurai, H. Schaffner, T. Shimoda, J. Taprogge, Zs. Vajta, V. Werner, J. Wu, A. Yagi, and K. Yoshinaga, Nucl. Instrum. Methods Phys. Res., Sect. B **317**, 649 (2013).

[17] S. Agostinelli *et al.*, Nucl. Instrum. Methods Phys. Res., Sect. A **506**, 250 (2003).

[18] J. Eberth, H. G. Thomas, P. v. Brentano, R. M. Lieder, H. M. Jäger, H. Kämmerling, M. Berst, D. Gutknecht, and R. Henck, Nucl. Instrum. Methods Phys. Res., Sect. A **369**, 135 (1996).

[19] W. Urban, W. R. Phillips, N. Schulz, B. J. P. Gall, I. Ahmad, M. Bentaleb, J. L. Durell, M. A. Jones, M. J. Leddy, E. Lubkiewicz, L. R. Morss, A. G. Smith, and B. J. Varley, Phys. Rev. C **62**, 044315 (2000).

[20] M. Wang, G. Audi, A. H. Wapstra, F. G. Kondev, M. MacCormik, X. Xu, and B. Pfeiffer, Chin. Phys. C **36**, 1603 (2012).

[21] http://www.nndc.bnl.gov/nndcscr/ensdf_pgm/analysis/logft/.

[22] E. Browne and J. K. Tuli, Nucl. Data Sheets **110**, 507 (2009).
[23] J. C. Hardy, L. C. Carraz, B. Jonson, and P. G. Hansen, Phys. Lett. B **71**, 307 (1977).
[24] O. Sorlin and M.-G. Porquet, Prog. Part. Nucl. Phys. **61**, 602 (2008).
[25] W. Urban, A. Korgul, T. Rząca-Urban, N. Schulz, M. Bentaleb, E. Lubkiewicz, J. L. Durell, M. J. Leddy, M. A. Jones, W. R. Phillips, A. G. Smith, B. J. Varley, I. Ahmad, and L. R. Morss, Phys. Rev. C **61**, 041301 (2000).
[26] ENSDF database; http://www.nndc.bnl.gov/endf/.
[27] C.-B. Moon, AIP Adv. **4**, 041001 (2014).
[28] N. Shimizu, T. Otsuka, T. Mizusaki, and M. Honma, Phys. Rev. C **70**, 054313 (2004).
[29] S. Sarkar, M. Saha Sarkar, Phys. Rev. C **78**, 024308 (2008).